Modelling of Soot formation in a Turbulent Diffusion flame using a comprehensive CFD-PBE model with full chemistry

P. Akridis, S. Rigopoulos*

Department of Mechanical Engineering, Imperial College of London, UK

Abstract

A discretised Population Balance Equation (PBE) model is coupled with a transported Probability Density Function (PDF) approach to simulate a turbulent methane non-premixed flame. The Lagrangian particle method is used in conjunction with k-ε turbulence model to solve the particle representations of mixture fraction, species, enthalpy and discrete sizes of soot number density. Full chemistry is considered via GRI1.2 mechanism. The optically thin radiation model and additional consumption/production terms are implemented according to soot kinetics. The PBE obtains the complete Particle Size Distribution (PSD) providing greater insight into soot formation.

Introduction

Soot is usually an undesirable combustion product with negative impact to human physiology and to the environment. Soot has been classified as a carcinogenic and mutagenic particulate matter causing adverse health effects [1]. Moreover, in a recent study, black carbon (a component of soot) is found to be the second major contributor to global warming behind carbon dioxide emissions [2]. Upon those reasons, new legislations are continuously reviewed in order to prevent a specific size and concentration of soot particles to be released in the atmosphere. This global awareness turned great attention in understanding and controlling soot formation. Thus, significant amount of research is conducted both experimentally and numerically.

Common practice is to explore the fundamentals of chemistry and complex soot kinetics in simple laminar flame systems before a turbulent case is considered. The implementation of soot and chemistry mechanisms is straightforward in laminar flames where no modelling is required to close the governing equations. Successful sooting and non-sooting laminar non-premixed flames with detailed chemistry can be found in [3]. Most of the practical devices operate in turbulent conditions where the flow field is chaotic. The complexity of soot and chemistry modelling is enhanced by fluctuations and their interactions. Furthermore, the wider length and time scales of mixing, chemical reactions and soot processes make a numerical investigation intractable when a Direct Numerical Simulation (DNS) or a Large Eddy Simulation (LES) is performed [4]. Therefore, effective computational models are sought to solve turbulent reacting flows with detailed chemistry and particle phenomena.

Reynolds-averaged Navier-Stokes (RANS) models are widely used in various Computational Fluid Dynamic (CFD) problems with decent accuracy at a reasonable numerical effort [4]. The RANS approach is used to solve the statistics of any turbulent quantity by averaging the transport equations and reducing significantly the dynamic range of scales. In combustion problems, Favre averaging is preferred due to strong density fluctuations. The drawback of this procedure is the difficulty to express accurately the highly averaged non-linear chemical reaction source term. An example is shown at [5] where the author computed finite-rate chemistry effects using Arrhenius modelling. The averaged reaction source term is modelled as an instantaneous source term represented by mean quantities (mean mass fractions, pressure and enthalpy) which essentially ignores the turbulent-chemistry interactions. Comparing the results with experimental, he concluded that ignoring these interactions lead in a perceptible loss of accuracy. The importance of turbulent-chemistry and turbulent-radiation interactions is also highlighted in [6]. To remedy this closure problem the RANS model is coupled with a transported Probability density function (PDF) approach. An alternative is coupling RANS with a laminar flamelet model and presumed PDF such as in [7] where the pdf shape distribution is assumed (e.g. β-pdf).

The benefit of using the transported PDF approach is that the chemical reaction, radiation emission and soot source terms appear in close form. The variances and the higher moments of all orders can be retrieved without any assumption on the pdf shape distribution. Several authors used this methodology successfully in turbulent sooting flames to capture the chemistry [8] and radiation interactions [6]. However, few terms on the PDF transport equation require closure as well and need external models to supply the turbulent time scale information, mean pressure and mean velocity fields. Several PDF formulations exist in the literature to attain closure such as composition, velocity-composition and velocity-composition-frequency. More modelling assumptions are required for the first method but is the easiest to implement and more robust on complex geometries than the other two [9].

PDF methods are a promising tool in turbulent combustion because the chemistry and soot kinetics can be incorporated without any modelling approximations. Despite those benefits, great amount of computational power is needed to solve the flame structure. Thus, in many turbulent combustion studies the chemistry is simplified and approximated instead of using time-consuming full chemical mechanisms with direct

* Corresponding author: s.rigopoulos@imperial.ac.uk

integration. Chemistry simplifications via systematically reduced or skeletal mechanisms or tabulation techniques are typically performed to speed up the computations [10]. Another major simplification is found in soot research. The PSD is routinely described by the evolution of two transport equations. These two equations are namely soot number density and soot mass fraction [11] which assume mono-disperse size distribution ignoring the polydispersity of soot particles. Only, recently the scientific interest has moved on from the mean properties of PSD to the morphology and detailed size distribution of soot particles [12].

In this paper an in-house CFD code is used in conjunction with a Lagrangian Monte-Carlo algorithm. To ensure its consistency a sophisticated particle tracking algorithm is applied. A discretised Population Balance Equation (PBE) model is coupled to the hybrid CFD/PDF method combined with a GRI 1.2 chemical mechanism in order to study the methane diffusion flame of Brookes and Moss [13]. The basics of this method have been introduced and discussed in [14] and [15]. The discretised PBE obtains the complete PSD without any prior assumption on the shape of the distribution. The radiation source term is implemented as an optically thin with additional species consumption and production terms that appear due to soot formation. Therefore, the scalar (composition) PDF approach of this paper treat the following particle representations as random variables, mixture fraction, species mass fractions, enthalpy and the discrete sizes of soot number density taking into account the polydisperisty of soot particles.

CFD –RANS code

The one point, one time scalar PDF method is coupled with a time-dependent RANS code and k-ε turbulence model. The CFD code is discretised by a finite volume scheme where the convection terms are treated with an upwind configuration and a Total Variation Diminishing (TVD) scheme. The averaged momentum and k-ε equations are solved in axisymmetric cylindrical configuration. A rectilinear grid is generated to represent the numerical 2D domain (radial and axial coordinates). The boundary conditions and the geometry of this domain are set according to the experimental specifications [13]. The CFD code supplies to the scalar pdf the mean velocity field and the turbulence time scale. The structured grid is used to estimate ensemble mean scalars in each computational cell which are required for the calculation of the micro-mixing term. Time-averaging solution is further used in each cell to reduce the statistical error. The following k-ε equations are solved to predict the turbulence spreading rate. They are shown in Cartesian tensor notation form and repeated indices imply summation.

$$\frac{\partial}{\partial t}\left[\bar{\rho}k\right]+\frac{\partial}{\partial x_j}\left[\bar{\rho}\tilde{u}_j k\right]=\frac{\partial}{\partial x_j}\left[\left(\mu+\frac{\mu_T}{\sigma_k}\right)\frac{\partial k}{\partial x_j}\right]+G-\bar{\rho}\varepsilon \qquad (1)$$

$$\frac{\partial}{\partial t}\left[\bar{\rho}\varepsilon\right]+\frac{\partial}{\partial x_j}\left[\bar{\rho}\tilde{u}_j \varepsilon\right]=\frac{\partial}{\partial x_j}\left[\left(\mu+\frac{\mu_T}{\sigma_\varepsilon}\right)\frac{\partial \varepsilon}{\partial x_j}\right]+\frac{\varepsilon}{k}\left[C_{\varepsilon 1}G-C_{\varepsilon 2}\bar{\rho}\varepsilon\right] \qquad (2)$$

The quantities with a bar on top are Reynolds averaged and the quantities with tilde are Favre averaged. The other terms are ρ which is the mixture density, μ is the molecular viscosity of the mixture, μ_T is the turbulent (eddy) viscosity, σ is the turbulent Prandtl number and G is the production of turbulent kinetic energy. The eddy viscosity term is computed by the following relationship

$$\mu_T=\bar{\rho}C_\mu\frac{k^2}{\varepsilon} \qquad (3)$$

It is well known that for axisymmetric configuration, the k-ε model does not predict accurately the turbulence spreading rate. All the model constants including Schmidt and Prandtl numbers that are normally used by default are shown in Table 1. In this study, the only modification to improve the turbulence prediction is that $C_{\varepsilon 2}$ constant is changed to 1.8 [4]. Several other corrections are proposed such as setting the constants listed in Table 1 with different values or functions of certain variables [11] depending on the type of the experiment. Moreover, a round jet correction source term could be added as it is shown by Pope in the turbulent dissipation rate equation [16].

Table 1: Standard Model constants

C_μ	$C_{\varepsilon 1}$	$C_{\varepsilon 2}$	σ_k	σ_ε
0.09	1.44	1.92	1.0	1.3

Lagrangian PDF method

The PDF equation is initially derived in an Eulerian form and can be found in [4]. Solving the joint pdf equation deterministically using finite difference techniques will result in a heavy computational expense. The computational time is increased exponentially with the number of independent scalars that are included. Hence, finite difference schemes are avoided and the Eulerian PDF is solved stochastically by an equivalent Lagrangian PDF formulation. The Lagrangian framework uses stochastic particles to represent the following quantities, mixture fraction, species mass fraction, total enthalpy and the discrete sizes (sections) of soot number density. A Monte-Carlo algorithm is adopted and the computational time is increased linearly with the addition of independent scalars. Thus, solving a large number of independent scalars with a Monte-Carlo algorithm is computationally feasible. The equation of dispersion of the notional particles in physical domain is shown below:

$$dx^{(P)}(t)=\left[\tilde{\mathbf{u}}+\frac{1}{\bar{\rho}}\nabla\Gamma_T\right]_{(P)}dt+\left[2\frac{\Gamma_T}{\bar{\rho}}\right]^{1/2}_{(P)}d\mathbf{W} \qquad (4)$$

Where W is an isotropic vector Wiener process and Γ_T is the turbulent diffusivity. Quantities with the symbol (P) denote the properties of a single Lagrangian particle.

The transport of those particle representations in the composition domain is estimated by using an appropriate mixing model such as Interaction by Exchange with the Mean (IEM), modified Curl model (CD) and the Euclidean Minimum Spanning Tree (EMST). In this study, the EMST model is applied which fulfills the localness criteria with mixing constant equals two. More information about this stochastic particle-interaction mixing model can be found in [17]. The transport in the scalar space is given by the equation below:

$$d\phi_a^{(P)}(t) = \Phi_{mix}^{(P)} + S_a^{(P)}dt + \delta_{rad}\frac{\dot{Q}_{rad}^{(P)}}{\rho^{(P)}}dt \quad (5)$$

Each mechanism is computed separately by using a time step operator splitting method. In eq. 5 the first term in the right hand side (RHS) is the micro-mixing term. The second source term represents the chemical reaction of each species and each soot size class (α=1, N_{sc}). The final source term is the radiation by emission. It is worth pointing out that the molecular diffusivity of soot particles in the laminar studies is usually omitted [3] due to insignificant contribution. Here, the PDF formulation implies the assumption of equal diffusivities for all scalars. Thus, in this study, the micro mixing term is the same for all soot particle sizes and gas-species. It should be kept in mind that neglecting differential diffusion may result in some inaccuracy. The Lagrangian PDF method in the end computes the ensemble mean density which is then time-averaged and returned to the RANS code in order to close the remaining terms.

Discretised PBE & Soot Kinetics & Radiation Model

Through the PDF approach, the source terms of the PBE are closed and do not require any modelling. A discretised PBE model via a finite element technique is introduced with exhaustive benchmarking in [18]. Particle volume is chosen as the only internal coordinate of the PBE where the entire size volume spectrum is covered by using an exponential grid. The PBE is capable of including coagulation mechanism as well but it is not considered in this case. Therefore, only growth/oxidation and nucleation mechanisms are presented resulting in the following partial differential equation.

$$\frac{\partial n(v,t)}{dt} = -\frac{\partial}{\partial v}\left(G(v)\cdot n(v,t)\right) + B_0(N_0)\delta(v-v_0) \quad (6)$$

The first term is the accumulation term on the left hand side (LHS) of eq. (6). The first term on the RHS of eq. (6) is the convection of soot particles in the size space by growth and oxidation kinetics. The last term is the nucleation mechanism where δ is the kronecker delta.

An acetylene based soot model is applied. Nucleation and surface growth terms are first order dependent on acetylene molar concentration whereas oxidation is dependent on molecular oxygen and hydroxyl concentrations. No aggregation or coagulation is applied to this study considering the conclusions in [3]. A major assumption is that the shape of soot particles is considered to be spherical. All soot formation processes are highly dependent on temperature. Thus, a good estimation of temperature and the important aforementioned species are needed to achieve a good prediction.

Nucleation rate: $$N_0 = \frac{2N_A k_n(T)\left[C_2H_2\right]}{C_{\min}} \quad (7)$$

Growth rate: $$G_{SG} = \frac{2k_{HW}(T)\left[C_2H_2\right]A_s}{\rho_s} \quad (8)$$

Oxidation Rates:

$$G_{O_2} = \frac{120\left[\frac{k_\alpha X_{O_2}\chi_1}{1+k_z X_{O_2}} + k_b X_{O_2}(1-\chi_1)\right]A_s}{\rho_s} \quad (9)$$

$$G_{OH} = \frac{\frac{167X_{OH}}{\sqrt{T}}A_s}{\rho_s} \quad (10)$$

In eq. (7) the reaction rate constant, k_n, is a function of Temperature, T. C_{min} is the minimum number of carbon atoms that is required to produce an incipient soot particle. It is assumed to be 700 carbon atoms [3] with an initial soot particle diameter of 2.4 nm. N_A is the Avogadro constant. Nucleation rate and the surface growth rates are dependent on acetylene molar concentration denoted by brackets. The soot density, ρ_s is defined 1800 kg/m^3 and A_s is the surface area of an individual section of particles. X variables denote mole fraction of a species. The nucleation reaction rate constant can be found in [3] whereas all the other surface growth and oxidation reaction rate constants are set according to [19, 20].

The radiation model is assumed to be optically thin where the gas-species and soot particles only emit radiation and do not re-absorb any energy. The following equation is implemented to take into account the radiation of the following species CH_4, H_2O, CO and CO_2. The absorption coefficients are calculated from the RADCAL program and are shown in TNF workshop website [21].

$$\dot{Q}_{rad} = 4\sigma\left(T^4 - T_b^4\right)\sum_{i=1}^{Nsp} p_i a_{p,i} \quad (11)$$

The σ is the Stefan-Boltzmann constant, T_b is the background temperature of the experiment and N_{sp} is the total number of species. Partial pressure of each species is denoted by p_i and α is the absorption coefficient. The equation for radiation of soot particles is similar to eq. (11) where instead of a fourth dependence on temperature it has a fifth dependence and the absorption coefficient is defined as $\alpha_{soot} = 1307 f_v$ where f_v is the soot volume fraction according to [8].

Computational domain – Methane Experiment

In this study the weakly sooting atmospheric methane flame of Brookes and Moss [13] is investigated. Methane chemistry is well known and good choice for analysis. This is an axisymmetric piloted non-premixed flame where centerline and radial measurements are taken for the mean quantities of mixture fraction, temperature and soot volume fraction. The experiment consists of a jet burner with 4.07 mm diameter issuing pure methane with a bulk velocity of 20.3 m/s and jet exit Reynolds number of 5000. A small annular pilot is used to stabilise the flame. The pilot and the central fuel tube are surrounded by an air co-flow with an approximate uniform velocity of 0.5 m/s. The experiment is at atmospheric pressure and the inlet temperature is 290 K for both the fuel and the oxidizer. This is a confined flame with a Pyrex tube internal diameter of 0.155 m.

The computational axisymmetric 2D domain is extended by 78 mm radially and 600 mm axially. During the experiment the visible flame length is observed to be around 600 mm [13]. Uniform inlet velocity profiles are set for the fuel and the oxidizer. Inlet and outlet boundary conditions are applied on the bottom and the top of the domain respectively. The two axial parallel planes are defined as symmetry boundary conditions. A non-uniform grid is applied with 50 points in radial and 80 points in the axial direction. The grid is finer towards the jet burner exit where larger gradients exist in that area. Additionally, 100 nodes are used to discretise the volume size domain of the PBE. The total number of scalars (N_{sc}) that is solved in the PDF is 134. Moreover, around 130 notional particles are used per cell to compute the evolution of the scalar variables of the PDF.

Results

Mean radial profiles of mixture fraction, temperature and soot volume fraction are compared for model validation. It should be noted that the scalar means are time-averaged with 3000 iterations to minimise the statistical error. This section starts with the comparison of mixture fraction along the centerline of the flame.

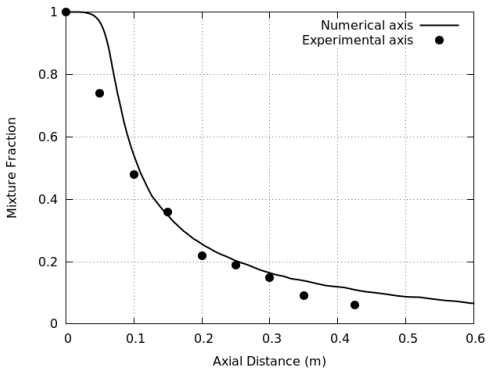

Figure 1: Centerline Mixture Fraction

The mixture fraction decay is captured well according to the experimental measurements. But near the burner the mixture fraction is over predicted. Possibly the mixing in that area is not computed accurately due to some uncertainties in the experimental boundary conditions. In Fig. 2 radial profiles at 250 mm above the burner are shown.

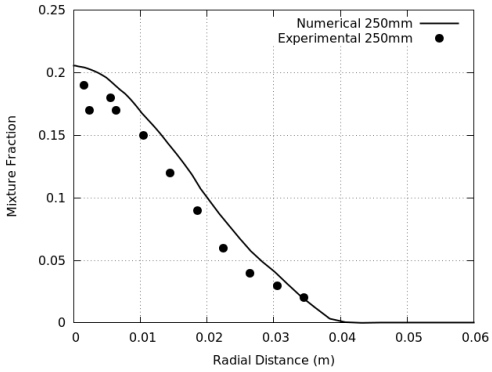

Figure 2: Mixture Fraction radial profile at 250 mm

Good prediction is observed for the mixture fraction profile in Fig. 2. The next Fig. shows the mixture fraction at 350 mm above the burner.

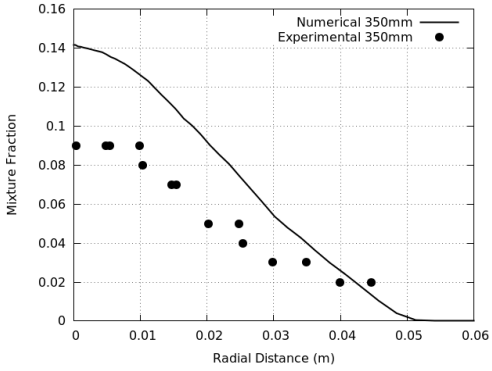

Figure 3: Mixture Fraction radial profile at 350 mm

A discrepancy between the mixture fraction profile and the experimental is easily seen starting from the centerline of the flame. Fig. 4 shows the temperature profile at the axis of the flame.

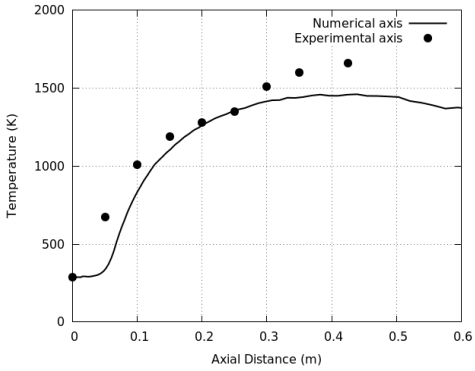

Figure 4: Centerline Temperature

Reasonable prediction is obtained for the temperature. Close to the jet burner exit under prediction is observed probably due to insufficient mixing of gas-species. Moreover, under prediction is shown after 0.3. This under prediction possibly is occurred by neglecting buoyancy and differential diffusion effects. Fig. 5 shows the radial temperature at 250 mm in the axial distance.

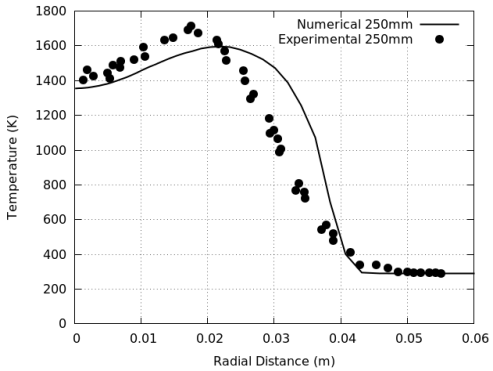

Figure 5: Temperature radial profile at 250 mm

Good prediction is achieved for the mean temperature radial profiles with a slight extended temperature profile between 0.02 and 0.04 m. Another radial temperature profile at 350 mm above the burner is shown in Fig. 6.

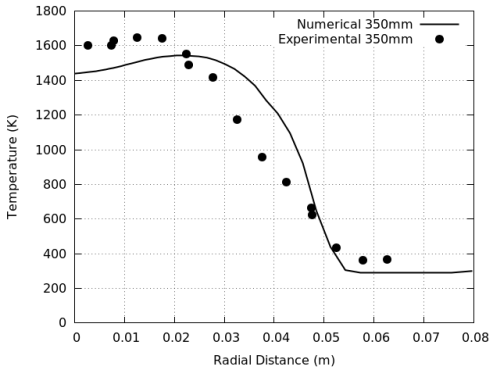

Figure 6: Temperature radial profile at 350 mm

Good agreement is observed for the temperature profiles on Fig. 6 where the same behavior is exhibited as in the previous Fig. 5. The next Fig. shows the soot volume fraction prediction on the centerline of the flame.

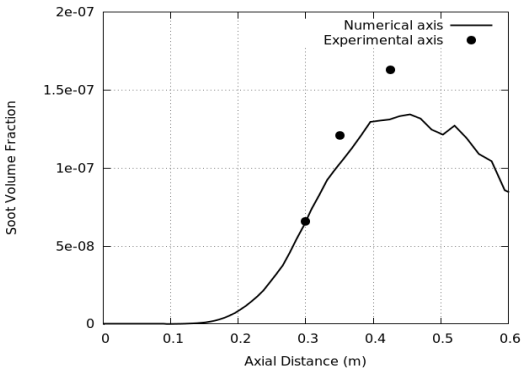

Figure 7: Centerline Soot volume fraction

Soot volume fraction or in other words the first moment of the PBE is well predicted. The peak soot volume fraction point is only slightly under predicted. The next Fig. shows the mean soot volume fraction radial profiles at 350 mm above the burner.

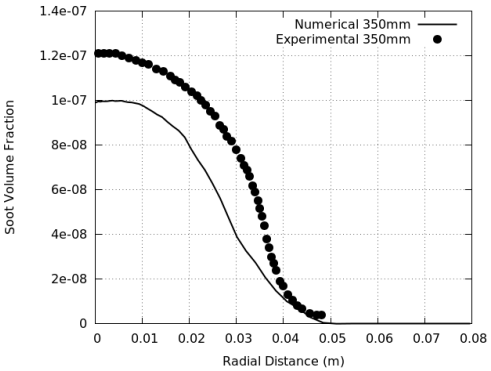

Figure 8: Soot volume fraction radial profile at 350 mm

By observing Fig. 8 near the axis the soot volume fraction is slightly under predicted but the behavior of the soot volume profile is similar to the experimental. The next Figs. show the PSD of soot particles on the centerline of the flame at three axial distances above the burner height. The PSD results are plotted in logarithmic scale and are normalized with their respective moments.

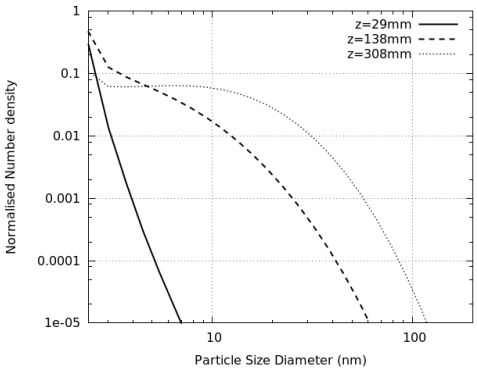

Figure 9: Normalised PSD (soot number density)

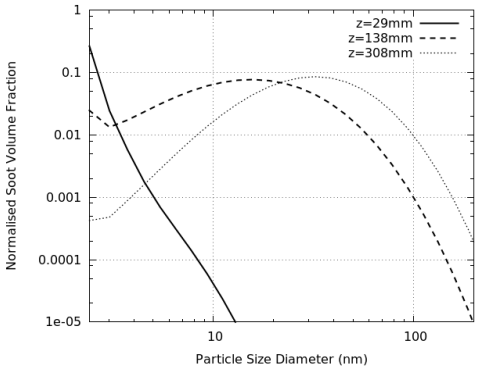

Figure 10: Normalised PSD (soot volume fraction)

By observing Figs. 9 and 10 the evolution of the complete PSD is shown in the axial direction. Incipient soot particles that exist near the burner height are growing as they move in the axial direction.

Conclusions

The polydispersity of soot particles is included to a turbulent methane diffusion flame by using a discretised PBE into a hybrid CFD/PDF model. Overall, the numerical results have reasonable agreement with the experimental and several improvements have been discussed in the previous section in order to achieve a better prediction. Unfortunately, no PSD measurements are obtained in this experiment to perform a comparison. With the combination of several soot kinetics from the literature, reasonable prediction is achieved for the mean quantities of mixture fraction, temperature and soot volume fraction centerline and radial profiles with few discrepancies in some points. Soot volume fraction is predicted on the same order of magnitude with the experimental measurements and the major characteristics are well captured.

Acknowledgments

The authors would like to acknowledge the EPSRC funding of this project.

References

[1] J. Singh, *Detailed soot modelling in laminar premixed flames*, Ph.D. thesis, University of Cambridge, 2006.

[2] T. C. Bond, S. J. Doherty, D. W. Fahey et al, J. Geophys. Res. Atmos. 118 (2013) 5380-5552.

[3] F. Liu, H. Guo, G. J. Smallwood, Ö. L. Gulder, Combust. Theory Modelling 7 (2003) 301-315.

[4] W. M. S. R. Weerasinghe, W. P. Jones, J. Turbulence 11 (2010) 1-37.

[5] Y. Zhang, *Hybrid particle/finite volume pdf methods for three dimensional time-dependent flows in complex geometries*, Ph.D. thesis, Pennsylvania State University, 2004.

[6] R. S. Mehta, D. C. Haworth, M. F. Modest, Combust. Flame 157 (2010) 982-994.

[7] S. J. Brookes, J. B. Moss, Combust. Flame 30 (1999) 486-503.

[8] R. P. Lindstedt, S. A. Louloudi, Proc. Combust. Inst. 30 (2005) 775-783.

[9] R. S. Mehta, *Detailed modeling of soot formation and turbulence-radiation interactions in turbulent jet flames*, Ph.D. thesis, Pennsylvania State University, 2006.

[10] D. C. Haworth, Prog. Energy Combust. Sci. 36 (2010) 168-259.

[11] A. Kronenburg, R. W. Bilger, J. H. Kent, Combust. Flame 121 (2000) 24-40.

[12] Q. Zhang, H. Guo, F. Liu, G. J. Smallwood, M. J. Thomson, Combust. Flame 32 (2009) 761-768.

[13] S. J. Brookes, J. B. Moss, Combust. Flame 116 (1999) 49-61.

[14] S. Rigopoulos, Chem. Eng. Sci 62 (2007) 6865-6878

[15] S. Rigopoulos, Prog. Energy Combust. Sci. 36 (2010) 412-443

[16] S. B. Pope, AIAA J. 16 (1978) 279-281.

[17] S. Subramaniam, S. B. Pope, Combust. Flame 115 (1998) 487-514.

[18] S. Rigopoulos, A. G. Jones, J. AIChE 49 (2003) 1127-1139.

[19] R. J. Hall, M. D. Smooke, M. B. Colket, in: R. F. Sawyer, F. L. Dryer (Eds.), Physical and Chemical Aspects of Combustion: A tribute to Irvin Glassman, in: Combustion Science and Technology Book Series, Gordon & Breach, New York, 1997, p. 189-230.

[20] M. D. Smooke, M. B. Long, B. C. Connelly, M. B. Colket, R. J. Hall, Combust. Flame 143 (2005) 613-628.

[21] N. Smith, J. Gore, J. Kim, Q. Tang, Available at http://www.ca.sandia.gov/TNF/radiation.html. [Accessed 26/12/2014].